

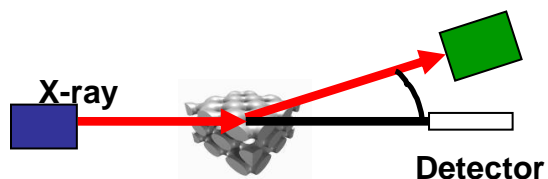
Definierte Porositäten - Mögliche positive Beeinflussung des Zellwachstums (?)

Prof. Bernd Smarsly,
Physikalisch-Chemisches Institut der JLU,
Heinrich-Buff-Ring 58,
35392 Gießen
bernd.smarsly@phys.chemie.uni-giessen.de

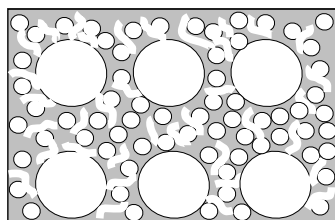
Overview

- ❖ Principles of the generation of mesoporous metal oxides
- ❖ Studies on the bioactivity of mesoporous materials (literature)
- ❖ The diversity of porosity and morphologies

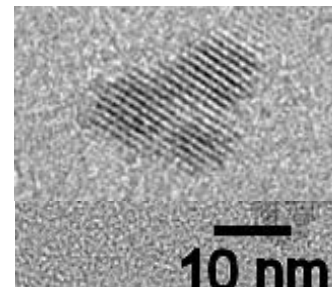
Characterization of nanostructures



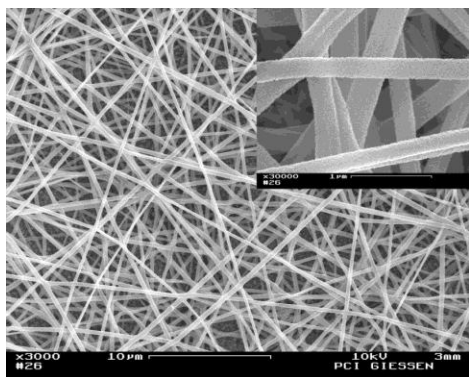
Multimodal pore structures



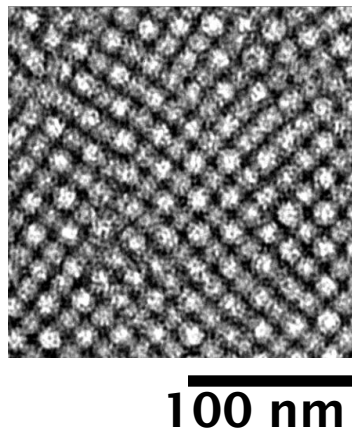
Nanoparticles



Electrospinning of inorganic nanofibers



Ordered nanoporous metal oxides



HPLC



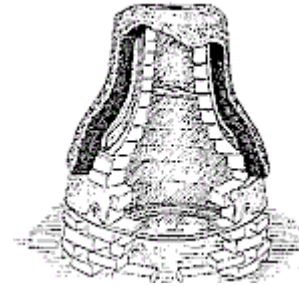
Applied electrochemistry



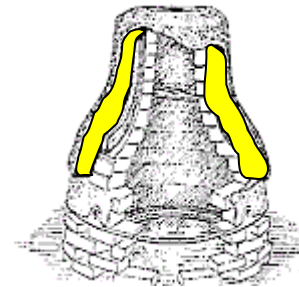
The principle of nanocasting



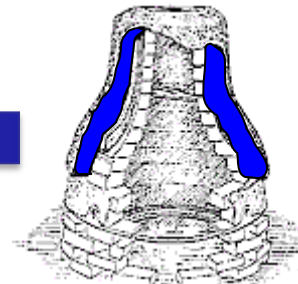
Petrified wood (Arizona, USA):



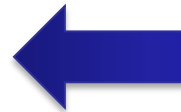
Wood



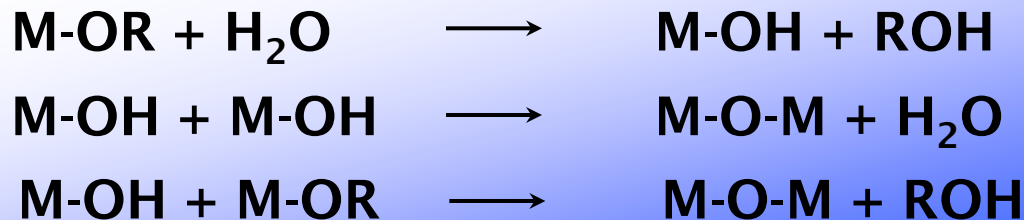
**Infiltration with
aluminosilicate
ions**



**Condensation
to 3D
aluminosilicates
(= mineral)**



Sol-Gel-Chemistry



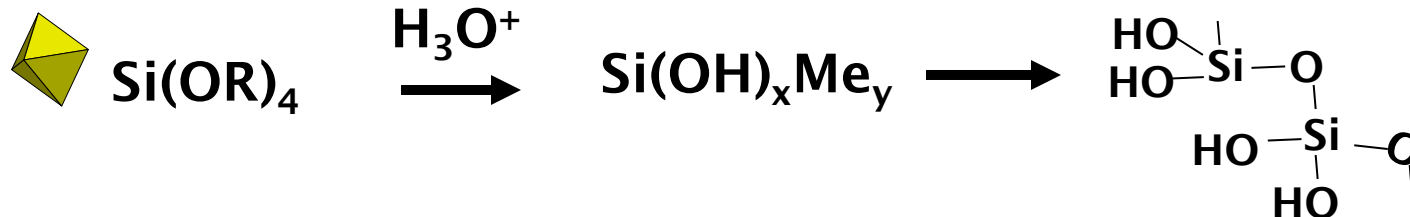
Hydrolysis: „SOL“

Condensation:
„GELIERUNG“

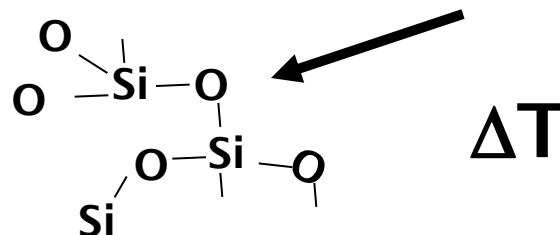
M-OR: z.B. $\text{Si}(\text{OMe})_4$

Hydrolysis

Condensed oxide
(Glas)

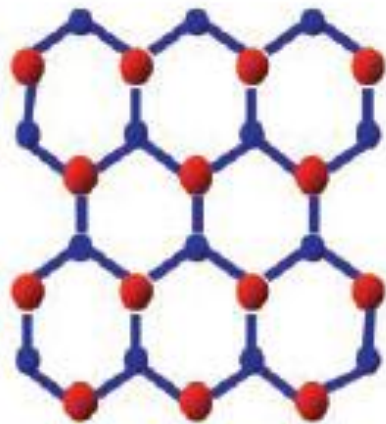


Metal oxide
(e.g. SiO_2 or TiO_2 , etc.)

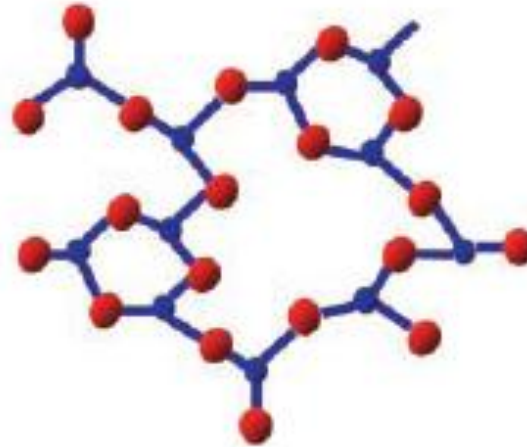


Structure of sol-gel derived SiO_2 networks

J. Chem. Soc., Dalton Trans., 2001, 97–108 97



SiO_2 network: ordered



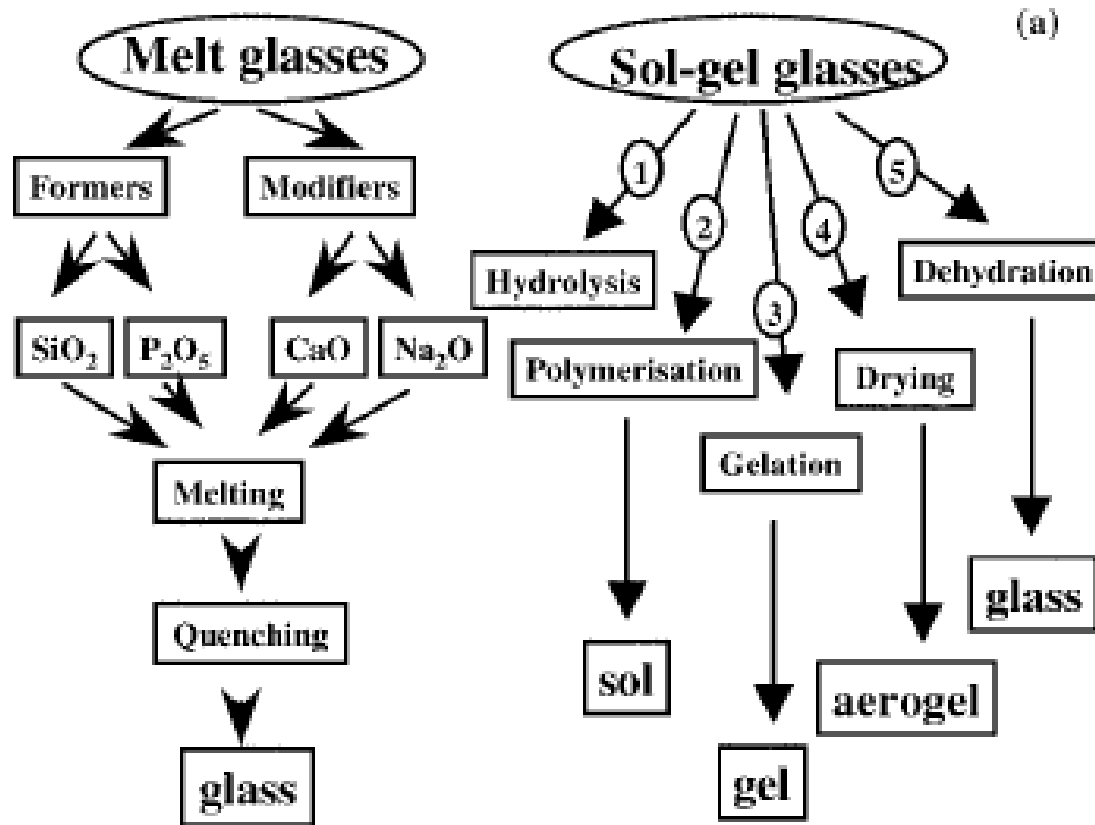
SiO_2 glassy network: disordered



Fig. 7 Two very different structural situations for an identical chemical composition, SiO_2 , namely ordered and disordered structure, thus giving rise to a crystalline ceramic and a glass, respectively.

Structure of sol-gel derived SiO₂ networks

J. Chem. Soc., Dalton Trans., 2001, 97–108 97



Structure of common glass

J. Chem. Soc., Dalton Trans., 2001, 97–108 97

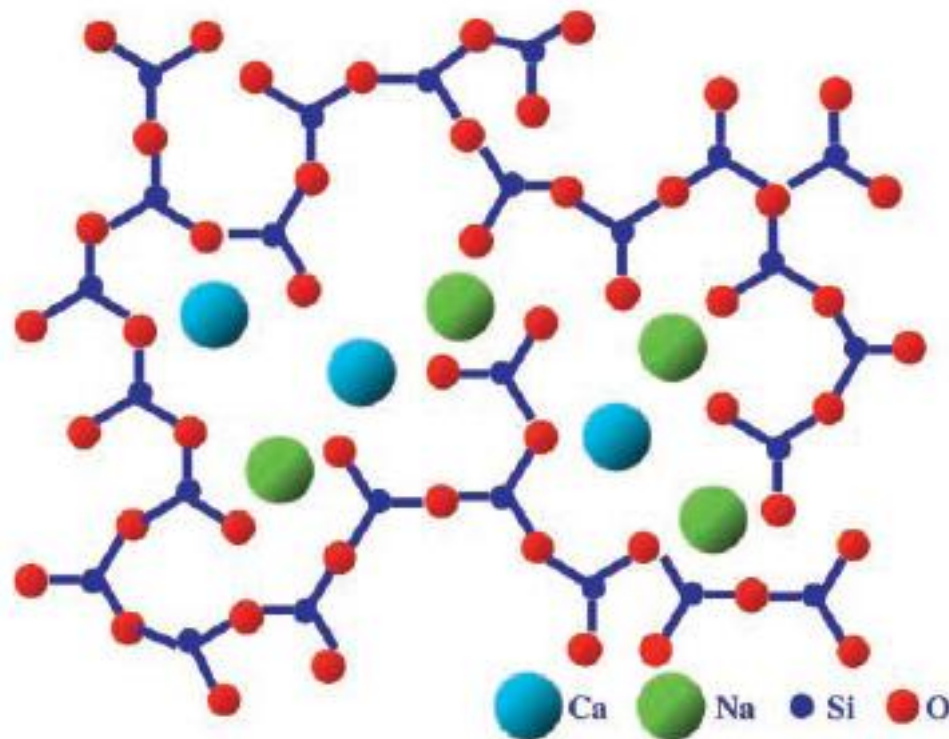


Fig. 9 Disordered structure of a glass in the $\text{SiO}_2\text{-CaO-Na}_2\text{O}$ system.

„Bottom-up“ principle for producing nanoscaled porosity



Building blocks

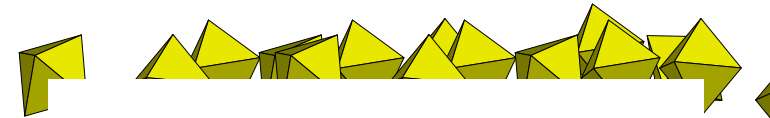


=

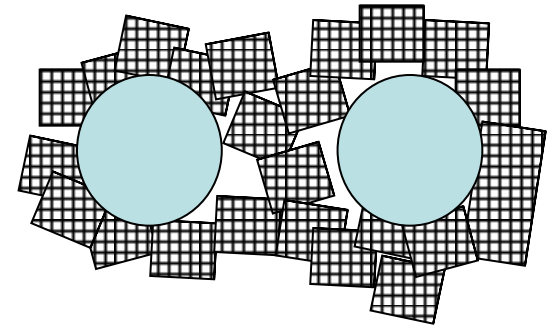
Molecular Precursor or nanoparticle



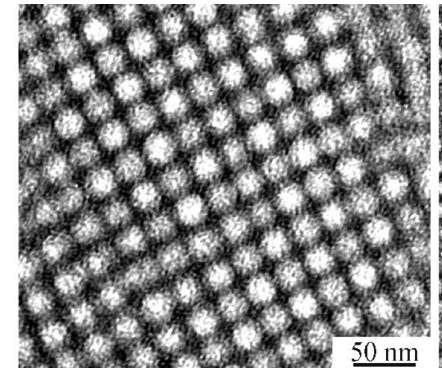
Construction (“Architect”)



condensation

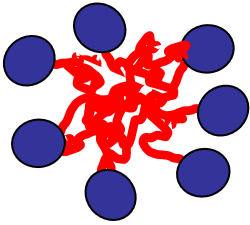


Building

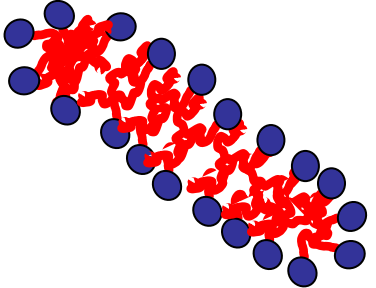


Template: Mesostructures of surfactants/block copolymers in solution

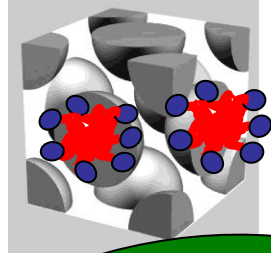
Dilute solution



Micelles

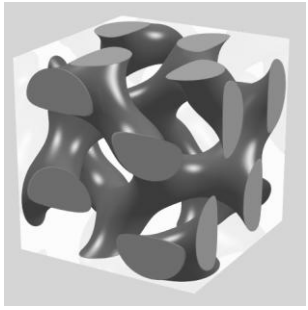
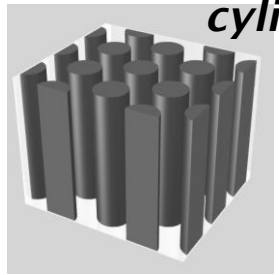


Cubic lattice



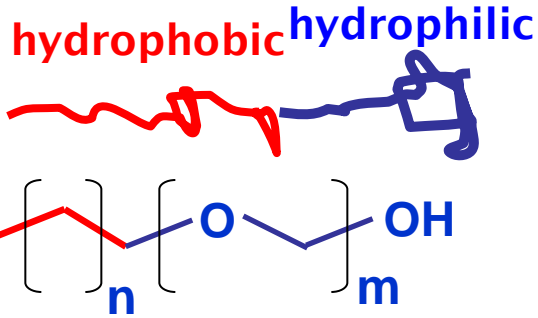
Lyotropic phases

2D hexagonal lattices of cylinders

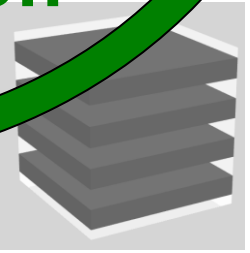


Gyroid

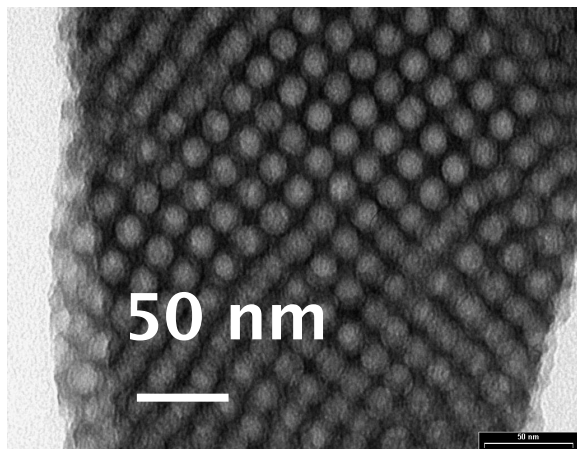
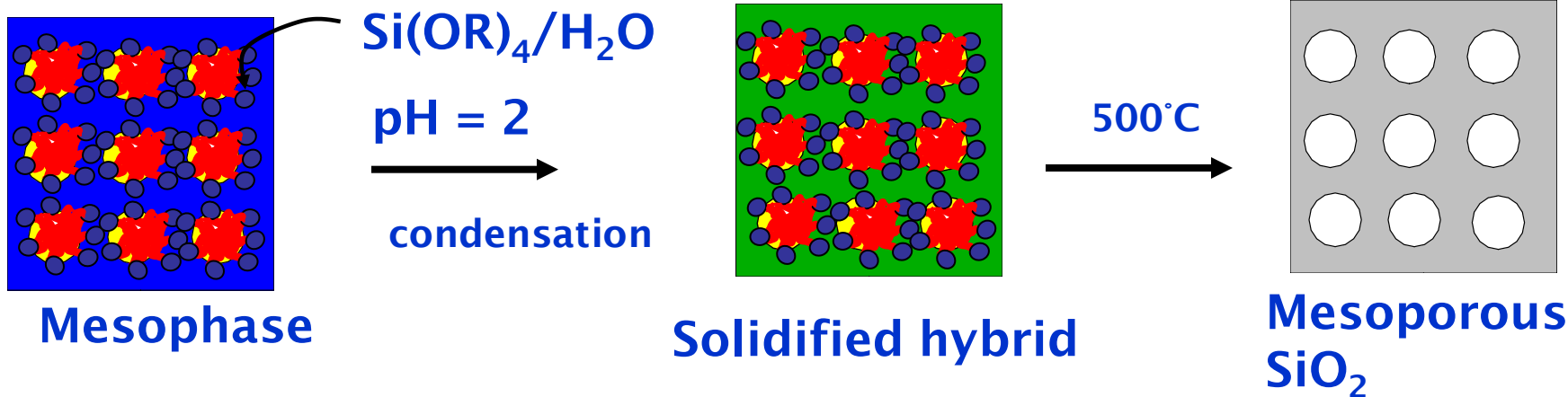
Concentration



Lamellae

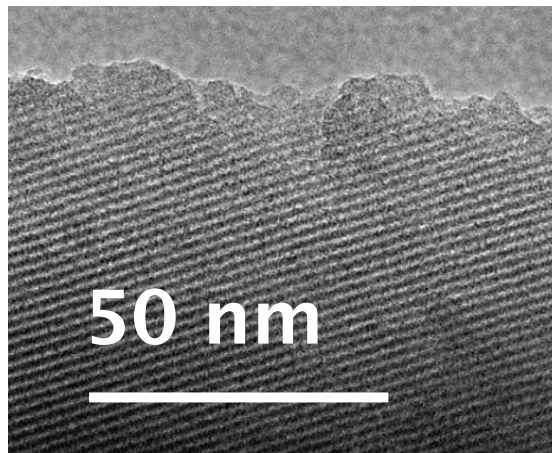


Nanocasting with block copolymers



Spherical mesopores
(14-40 nm)

Surface area ca. 90 - 200 m^2/g



Cylindrical mesopores
(3 nm - 8 nm)

Surface area ca. 500 - 900 m^2/g

AG Smarsly:

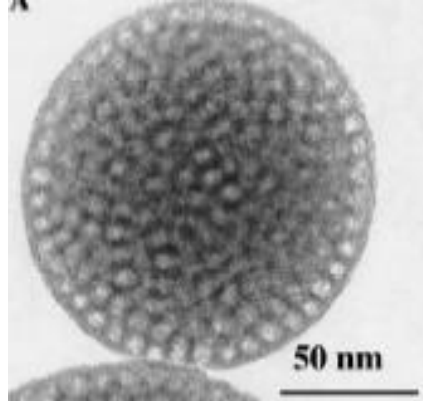
Large variability
of shape
and size
(3 nm - 40 nm)

Possible morphologies

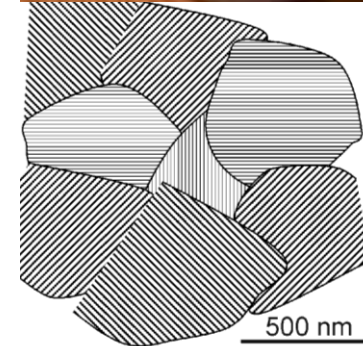
Thin films (50 – 1000 nm)



Mesoporous microparticles



Mesoporous powders



Mesoporous SiO₂ for bone tissue regeneration - 1

Vallet-Regi et al., J. Mater. Chem, 2006, 16, 26-31

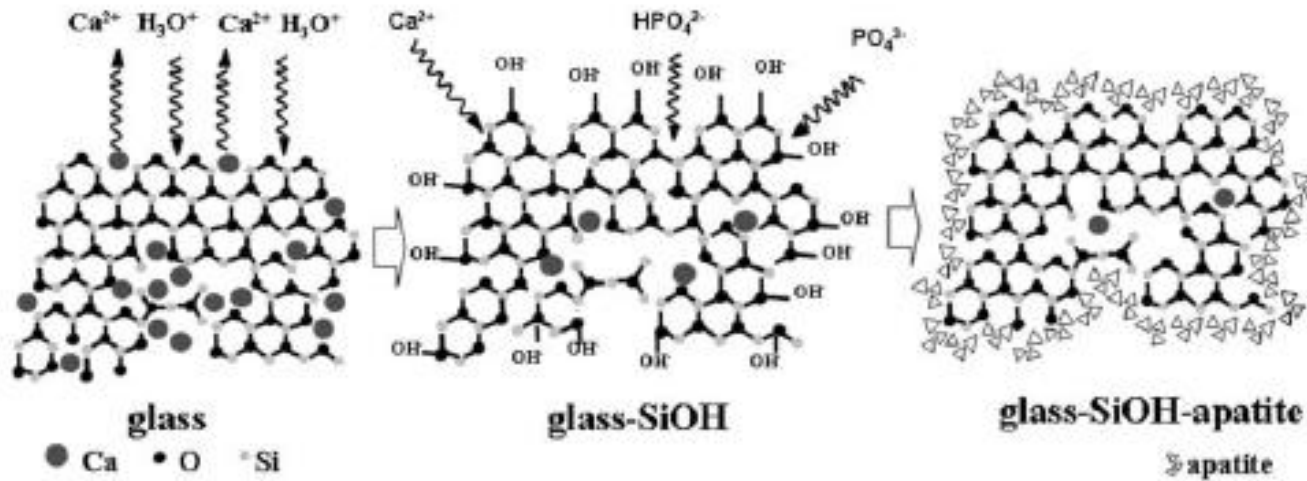


Fig. 2 Hydroxyapatite formation mechanism in bioactive glasses when soaked in physiological fluids.



Ionic co

	Na
SBF	142
plasma	142

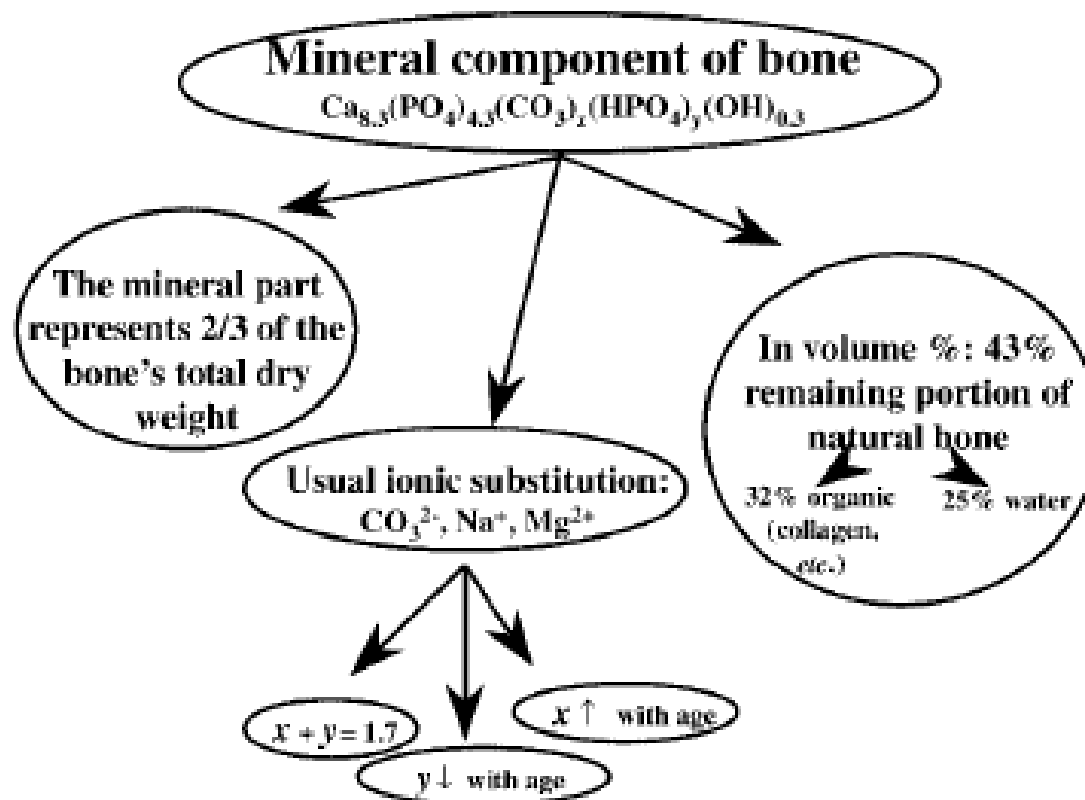


Fig. 6 Composition of the mineral component of bones.

Mesoporous SiO₂ for bone tissue regeneration - 1

Vallet-Regi et al., J. Mater. Chem, 2006, 16, 26-31

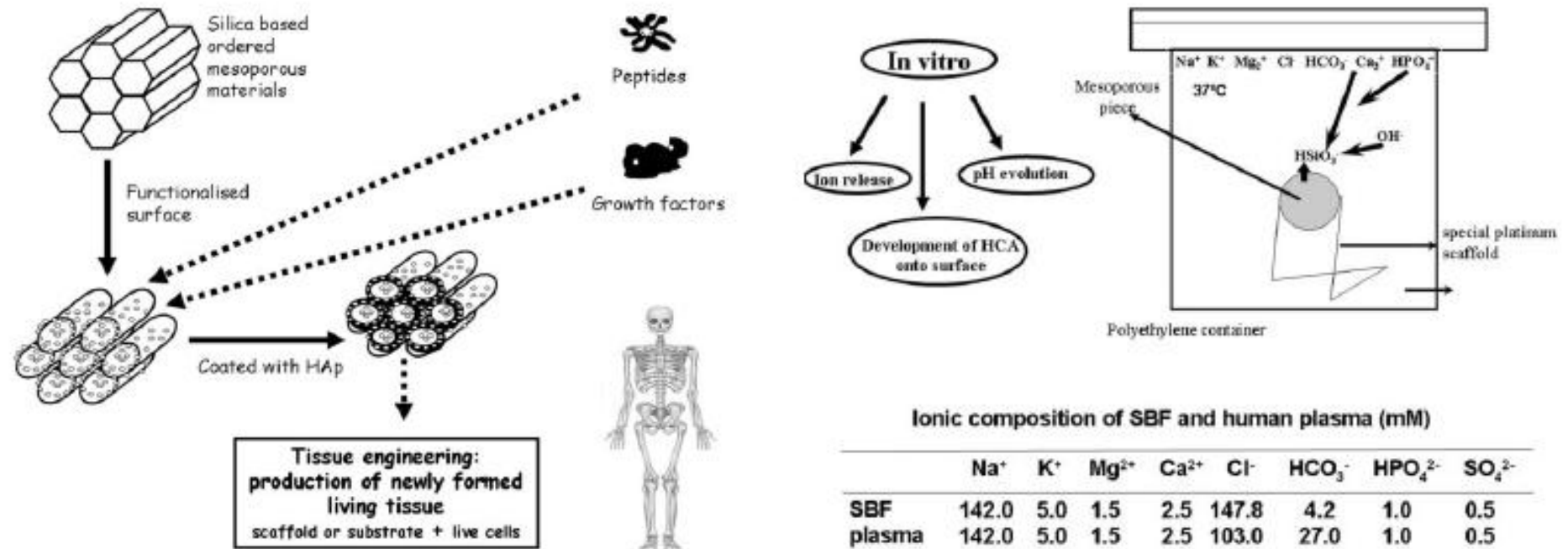


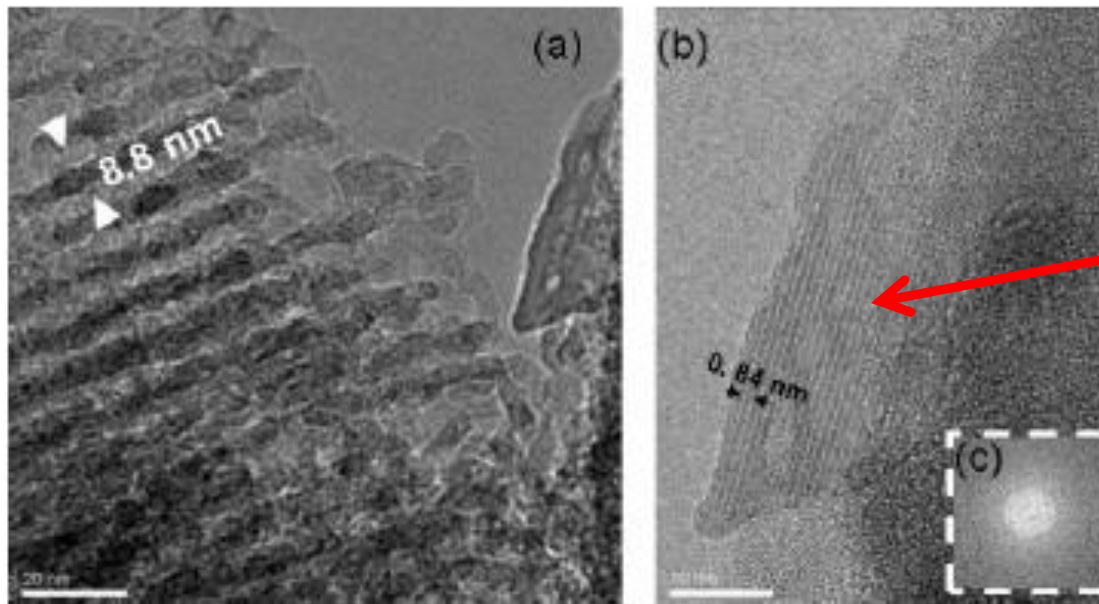
Fig. 7 Schematic illustration of tissue engineering technique promoted by bioactive ordered mesoporous materials which can be functionalized with organic groups and release different growth factors for tissue regeneration.

SBF: simulated body fluid

Mesoporous SiO₂ for bone tissue regeneration - 1

J. Mater. Chem, 2006, 16, 26-31

TEM analysis



apatite

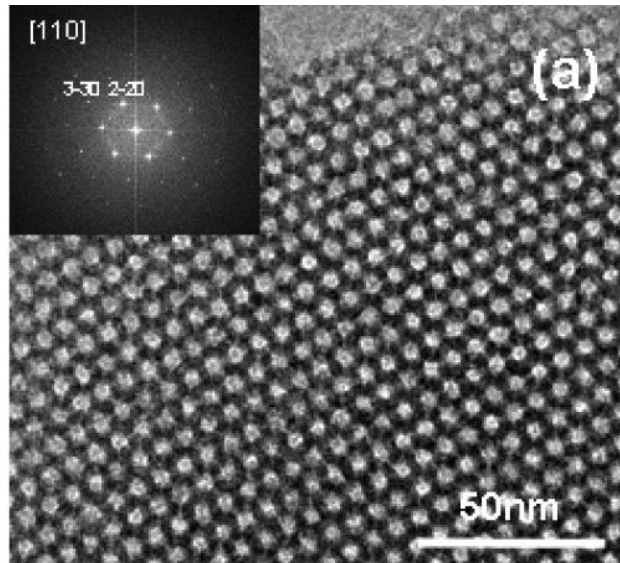
Fig. 6 TEM micrographs showing different features of SBA-15 after treatment: (a) area where the original mesoporous material is not completely transformed; features of both raw material and apatite are evident; (b) enhanced image reflecting the fact that apatite appears over the modified mesoporous material; (c) FT performed at the amorphous area in b.

Mesoporous SiO₂ for bone tissue regeneration - 2

Chem. Mater. 2006, 18, 3137–3144

Ordered Mesoporous Bioactive Glasses for Bone Tissue Regeneration

López-Noriega,[†] D. Arcos,^{*,†} I. Izquierdo-Barba,^{‡,§} Y. Sakamoto,[‡] O. Terasaki,[‡]
M. Vallet-Regí^{*,†}



**S85m:
3D
mesopore
structure**

Recipe:
Tetraethyl orthosilicate (TEOS), triethyl phosphate (TEP), and calcium nitrate, Ca(NO₃)₂, 4H₂O, (Aldrich) were used as SiO₂, P₂O₅, and CaO sources,

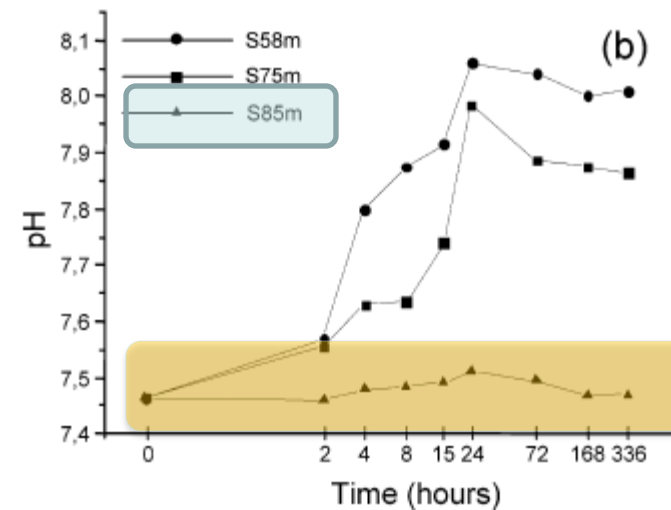
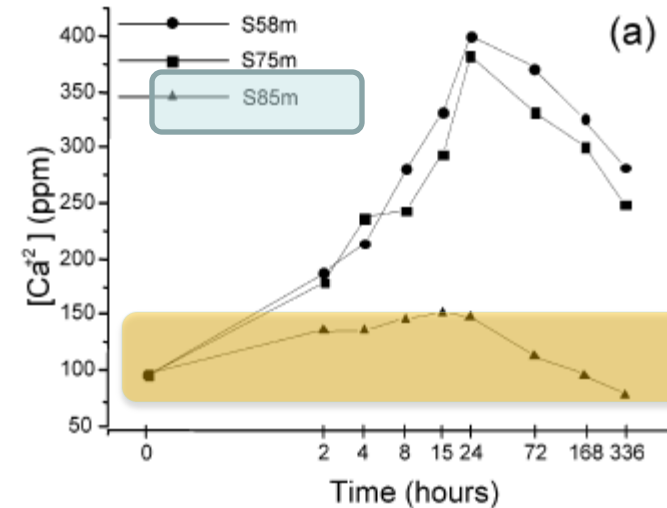


Figure 6. Variations of (a) calcium content and (b) pH values of the SB after soaking the mesoporous SiO₂-CaO-P₂O₅ glasses.

Mesoporous SiO₂ microspheres for bone grafting

Chem. Mater. 2009, 21, 1000–1009

Porous SiO₂ microspheres

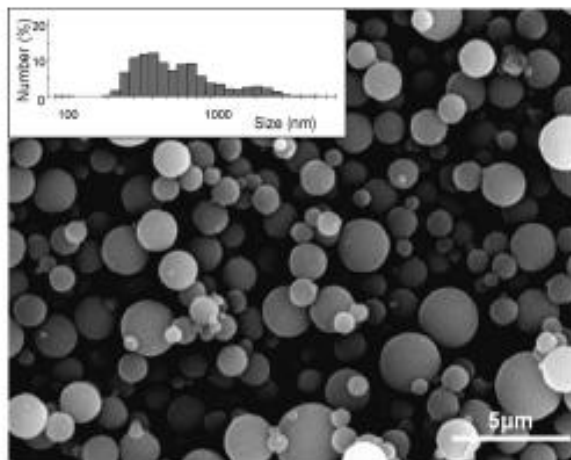


Figure 1. SEM micrograph of BMS85P. Magnification 5000 \times . Inset shows particle size distribution determined by DLS measurements.

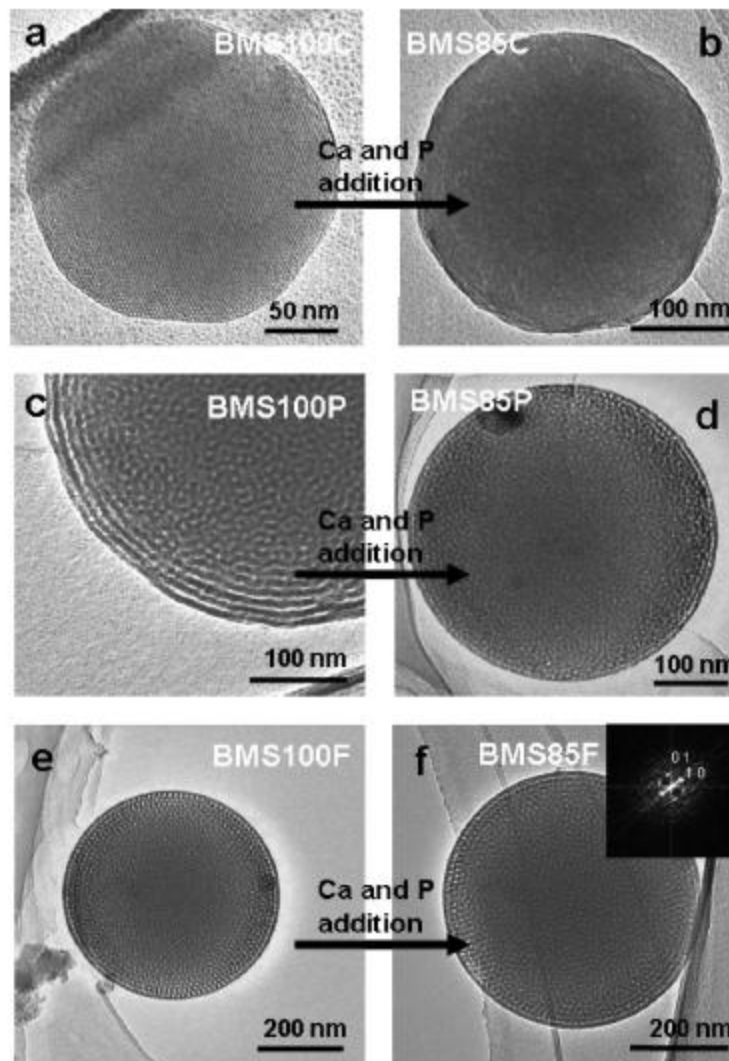
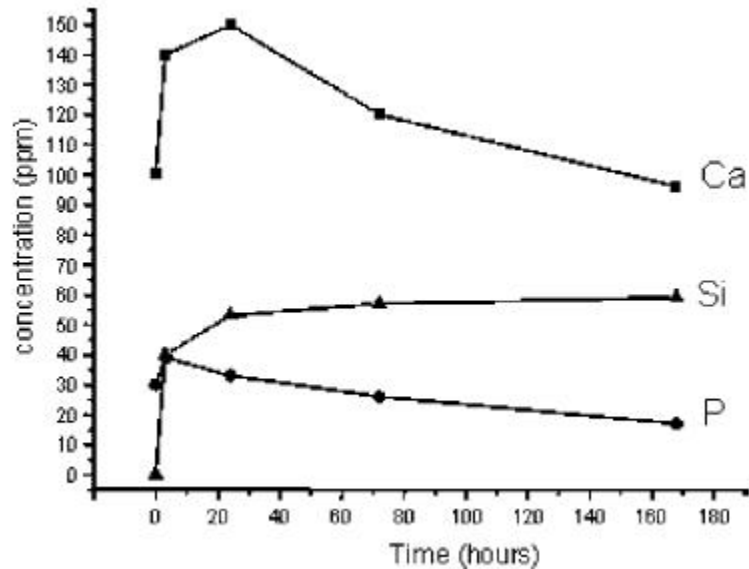


Figure 3. TEM images of BMS100x and BMS85x microspheres synthesized with CTAB, P123, and F127. Magnification 30 000 \times . Fourier transform pattern for BMS85F is shown, demonstrating the hexagonal mesoporous ordering remaining in this sample.

Mesoporous SiO₂ microspheres for bone grafting

Chem. Mater. 2009, 21, 1000–1009

Dissolution behavior



Spheres covered by apatite

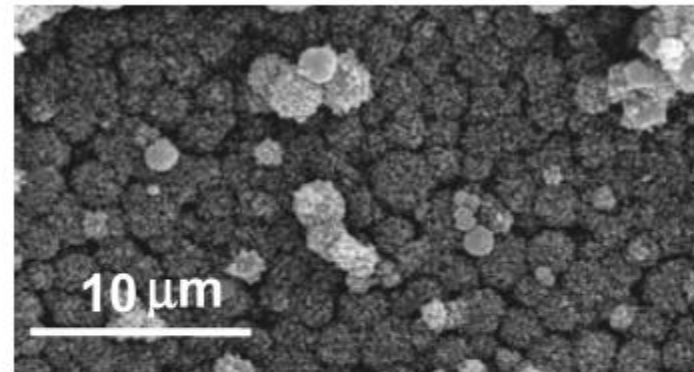


Figure 7. SEM micrographs of BMS85P after soaking in SBF for 3 days.



Modifications of apatite

High Specific Surface Area in Nanometric Carbonated Hydroxyapatite

Chem. Mater. 2008, 20, 5942–5944

S. Padilla,[†] I. Izquierdo-Barba,^{†,‡} and M. Vallet-Regí^(*,†,‡)

Synthesis of nanocrystalline, carbonated hydroxyapatite (CHA)

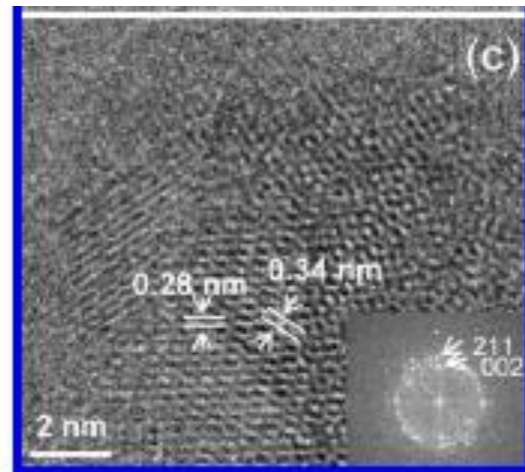
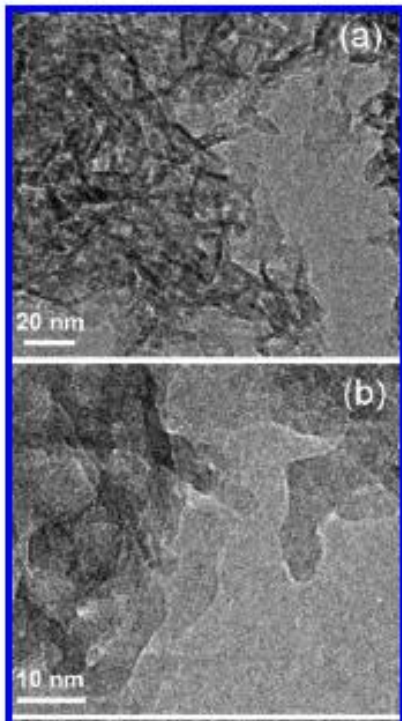


Figure 3. TEM images of CHA taken at different magnification (60 000, 300 000 and 600 000 K, respectively). (a, b) Low-magnification images show the small size and the needle-like shape of the nanoparticles. (c) HRTEM image and its corresponding Fourier diffractogram show the d -spacing corresponding to the 002 and 211 reflections of an apatite phase.

SiO₂ Aerogels for bone grafting

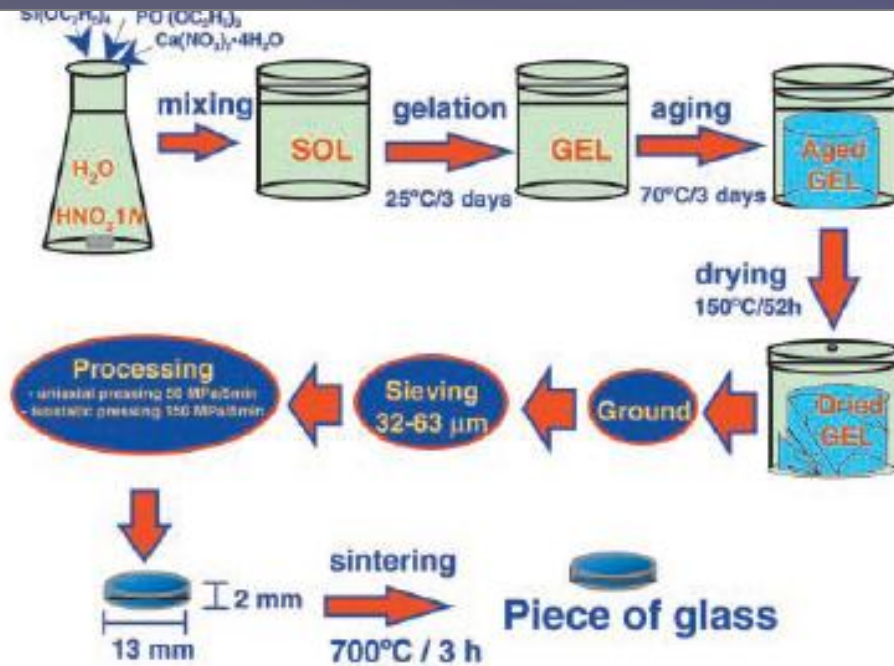
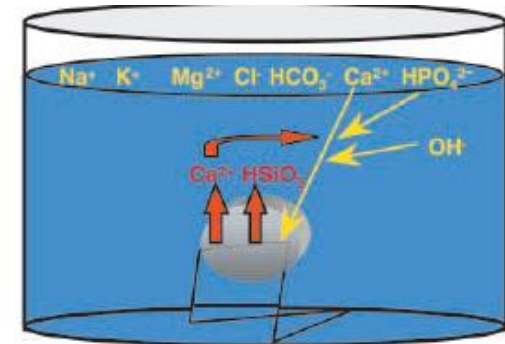


Fig. 10 Description of the synthesis process for bioactive glasses.



Ionic composition of SBF and Human Blood Plasma (mM)

	Na ⁺	K ⁺	Mg ²⁺	Ca ²⁺	Cl ⁻	HCO ₃ ⁻	HPO ₄ ²⁻	SO ₄ ²⁻
SBF	142.0	5.0	1.5	2.5	147.8	4.2	1.0	0.5
plasma	142.0	5.0	1.5	2.5	103.0	27.0	1.0	0.5

Fig. 15 Chemical process taking place between a bioactive glass and a solution of SBF.

In vitro bioactivity valuation

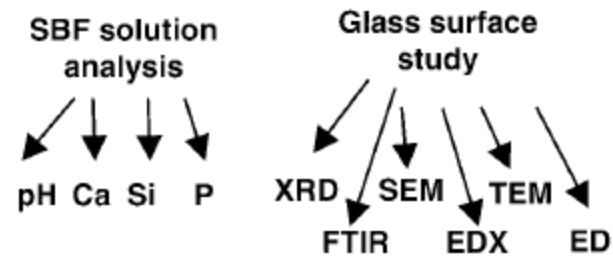
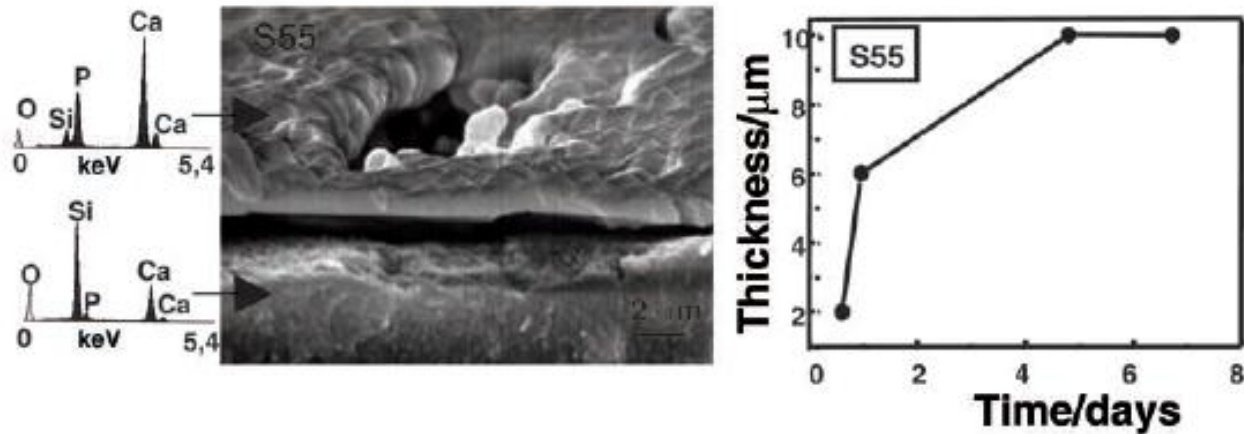


Fig. 14 Techniques employed in characterisation of bioactive glasses.

Modifications of apatite



. 20 Evolution with time of the apatite-like layer thickness on a bioactive glass. SEM and EDS techniques have been used.

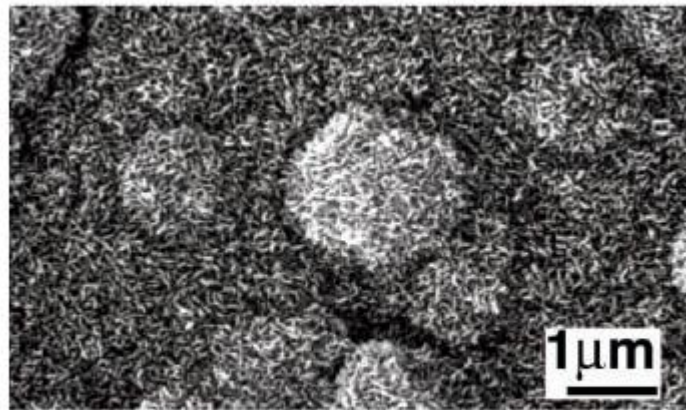


Fig. 18 Micrograph of a bioactive glass after soaking in SBF for one week.

Are nanoporous SiO₂ materials suitable?

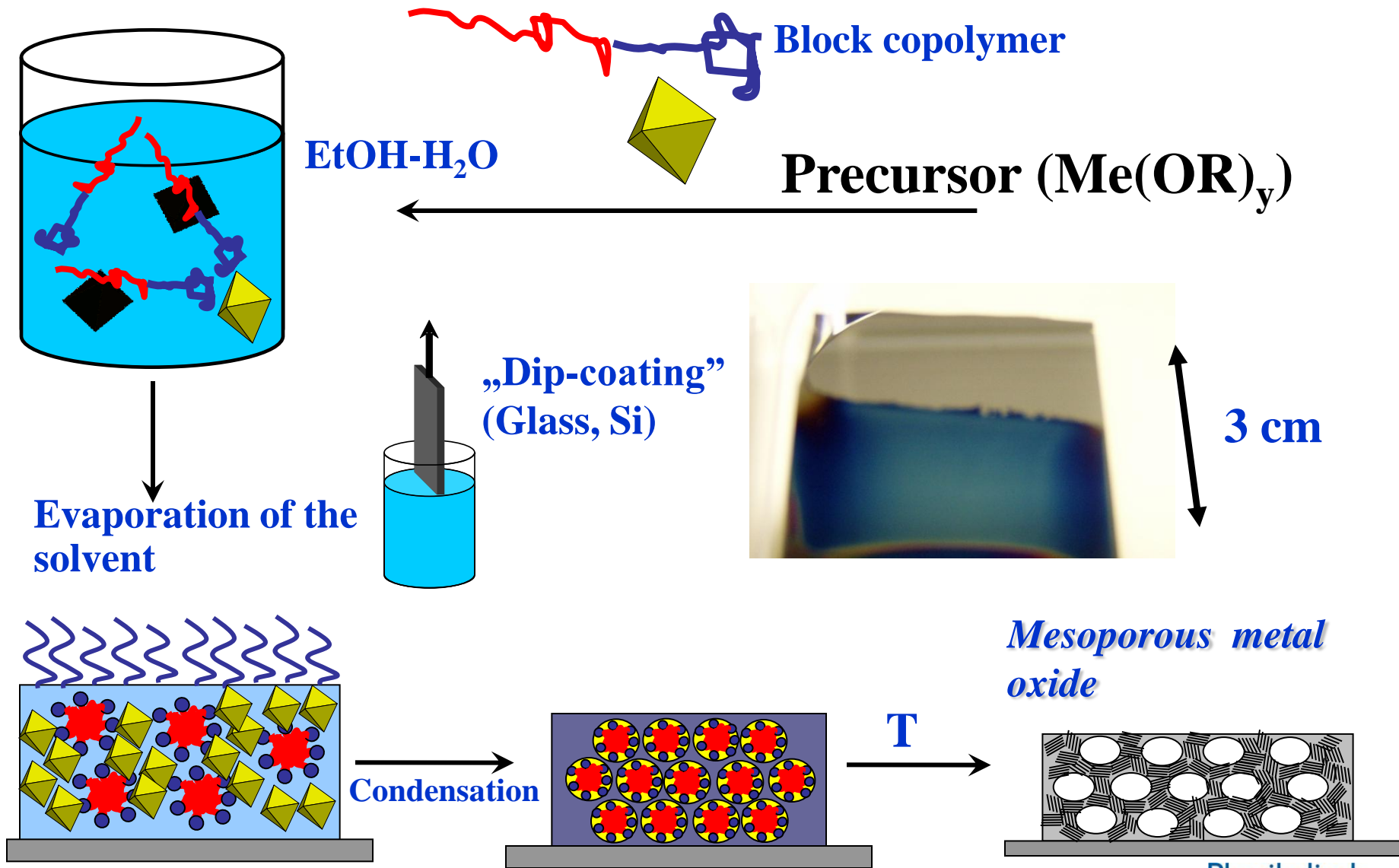
Problems of using porous SiO₂ as bioactive glass

- Mesoporous powders do not possess macroscopic shape, thus produce „ill-defined“ apatite layers
- The influence of the macroscopic shape is not understood
- Small mesopores (< 8 nm) can be easily blocked

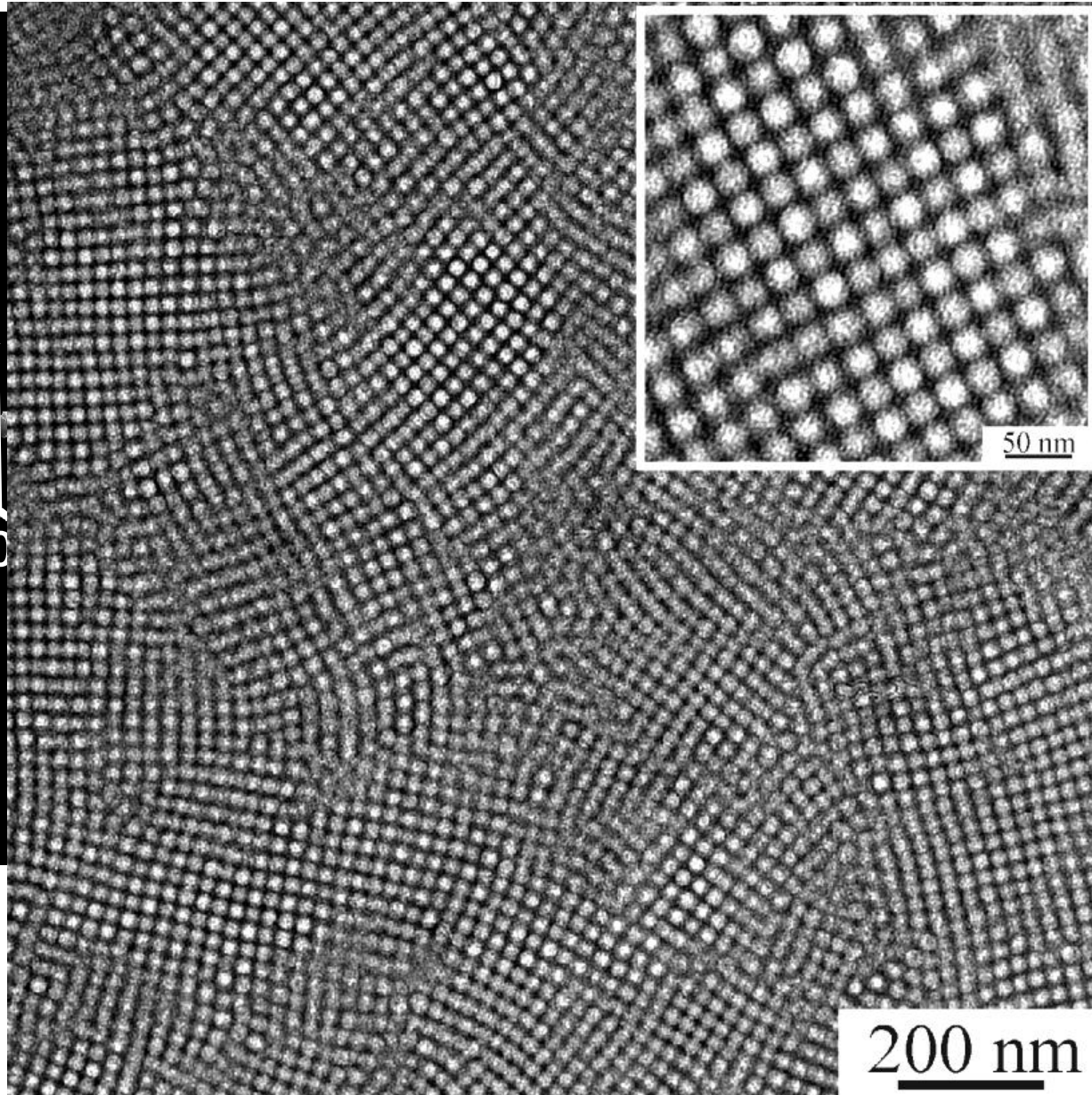
Possible requirements for the materials

- Well-defined shape (monoliths)
- Ideally: as little amount of SiO₂ as possible
- Combination of high surface area and high porosity

Mesoporous metal oxide films by „Evaporation-induced self-assembly” (EISA)



Macroscopic homogeneity

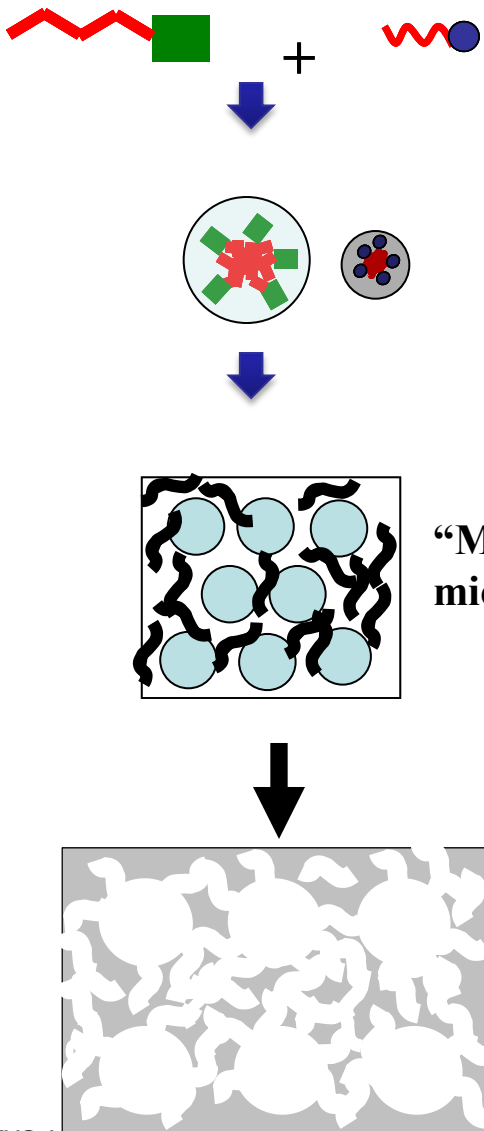


er-sized domains

Porosimetry)

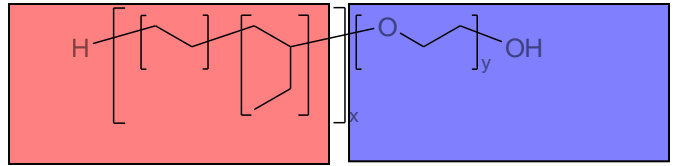
200 nm

Dual micellar templating

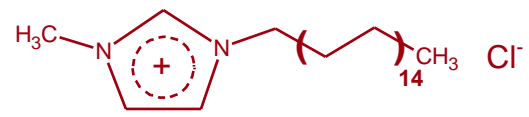


“Micellar mixing”/
micellar “alloys”

Large pores:
block copolymers or colloid particles

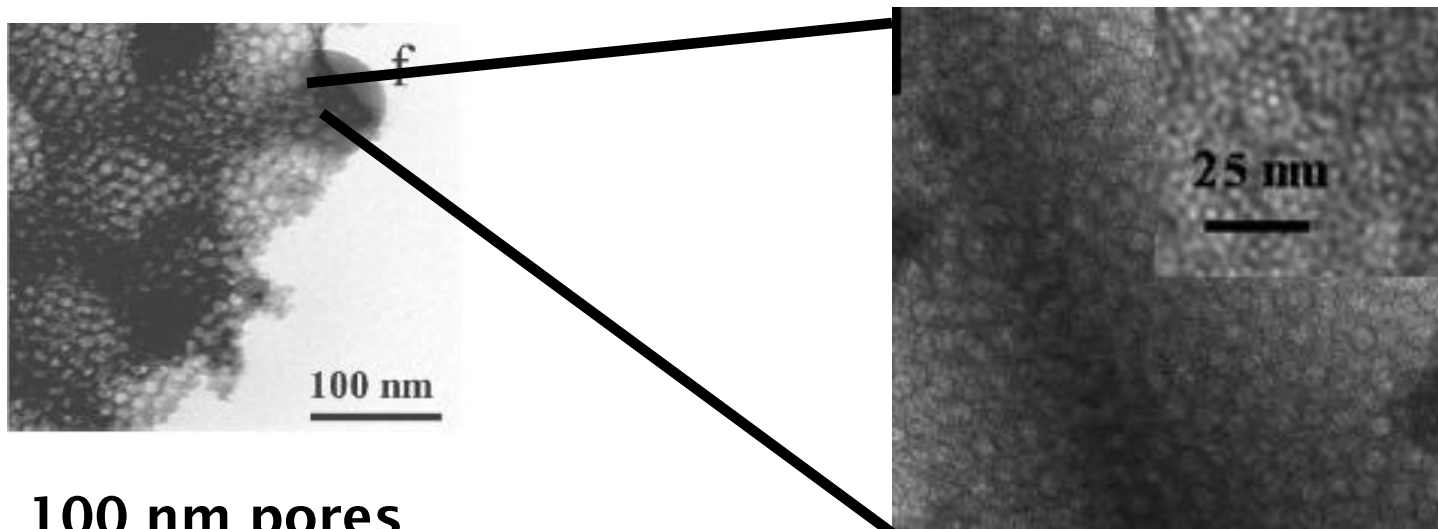


Small mesopores:
Small surfactants



Hierarchical pore structures

Combination of a large pore volume with large surface area

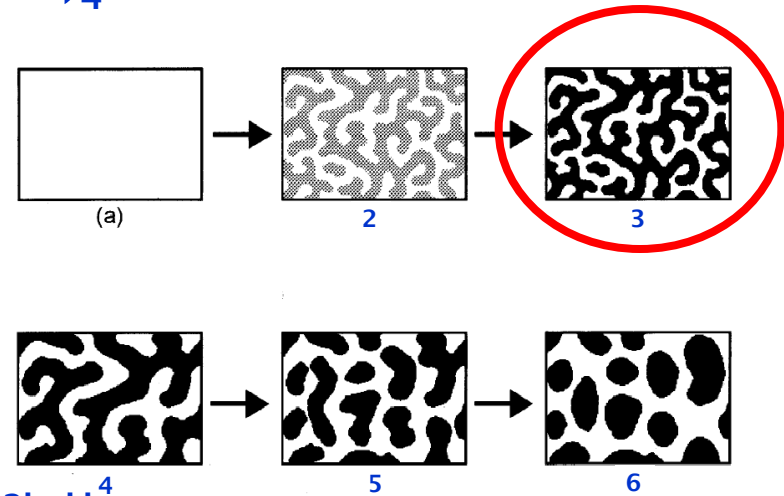
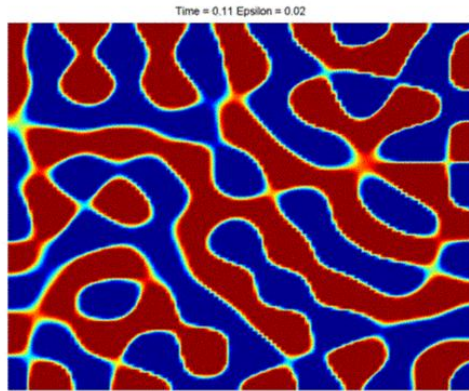


100 nm pores
+ 14 nm pores
+ 3 nm pores

Surface area: 600 m²/g
Pore volume: 1.3 ml/g

Generation of monolith pore structures: Nakanishi process

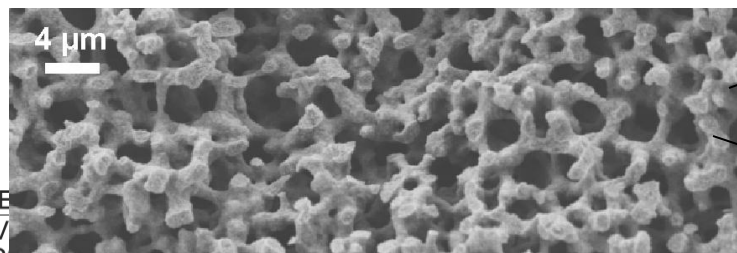
Sol-Gel-Prozess: PEO + "Si(OH)₄" + EtOH



<http://complex.gmu.edu/images/gallery/thumb/spinum2ind.jpg>

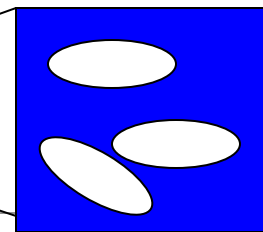
N. Ishizuka et al. (1998)

Meso- and macroporous SiO₂



5 - 20 nm

A double-headed arrow indicating a length scale of 5 - 20 nm.

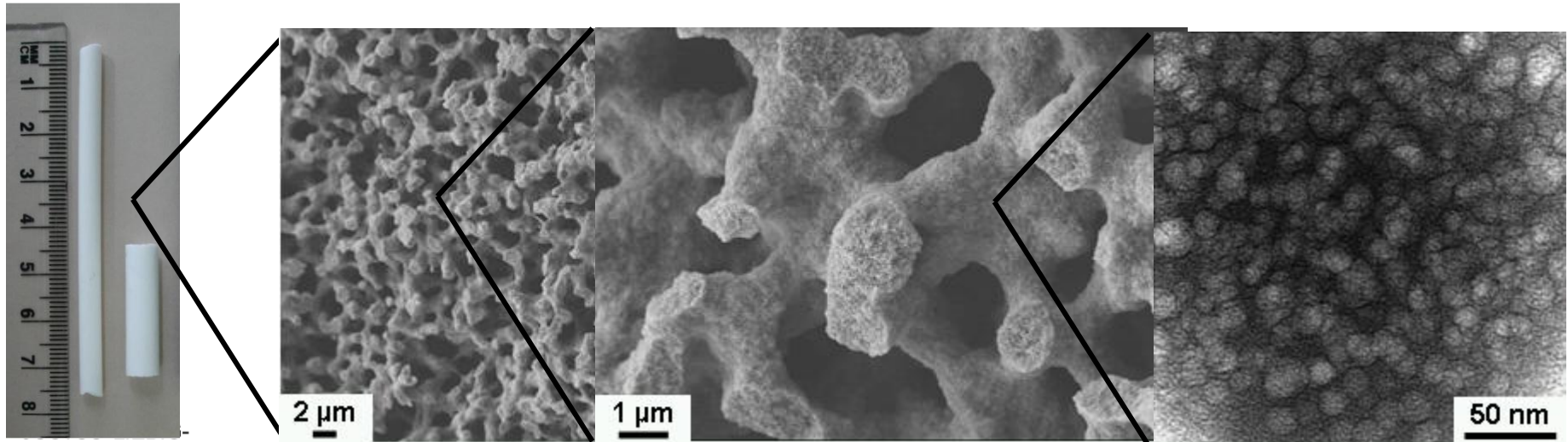


Structure of monolithic SiO₂ with hierarchical pore structure



- Shape control
- Large pores: 2-4 micrometer
- Mesopores: 13 nm
- Surface area: Ca. 250 m²/g
- Pore volume = ca. 0.8 ml/g

Electron microscopy



Application of monolithic SiO_2 in HPLC

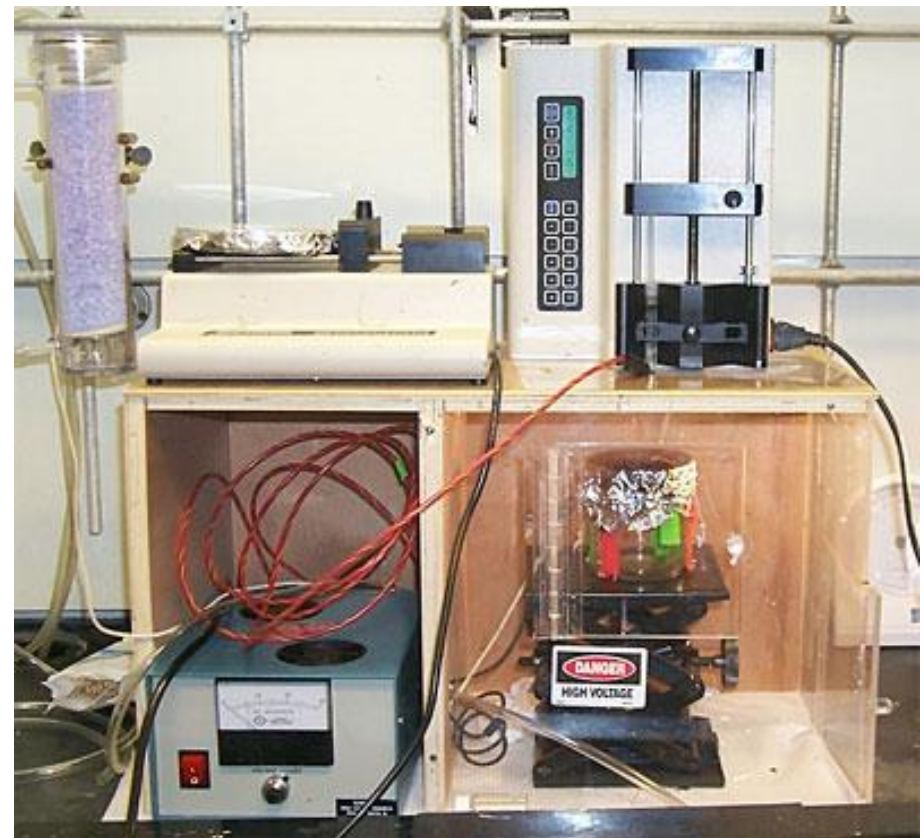
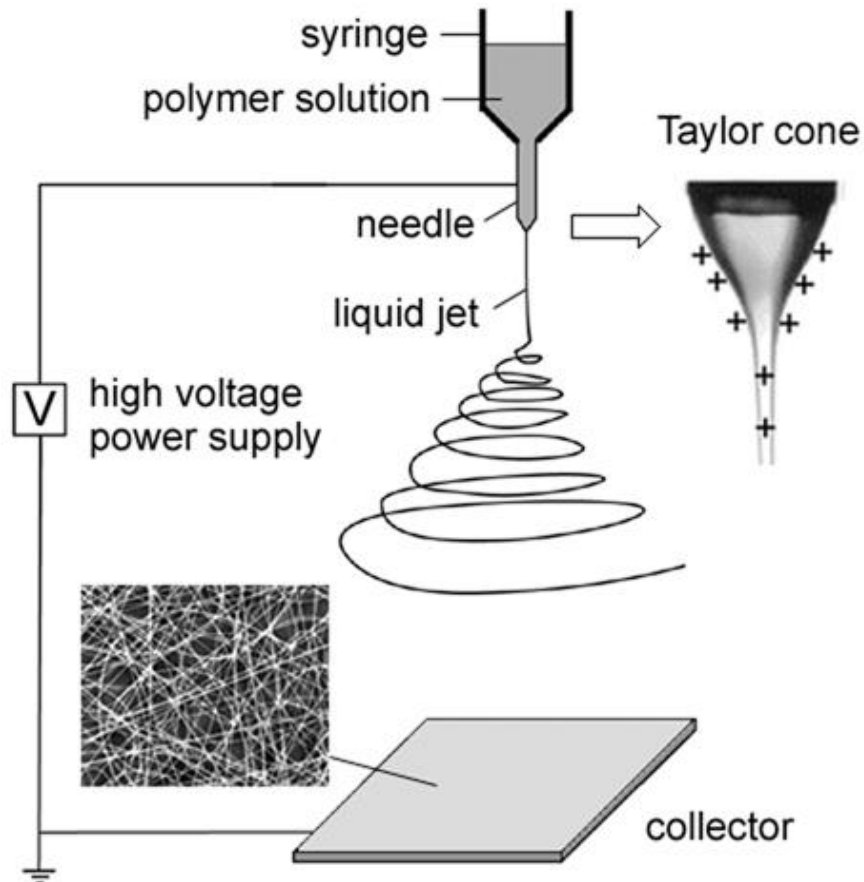


HPLC setup
AG Smarsly



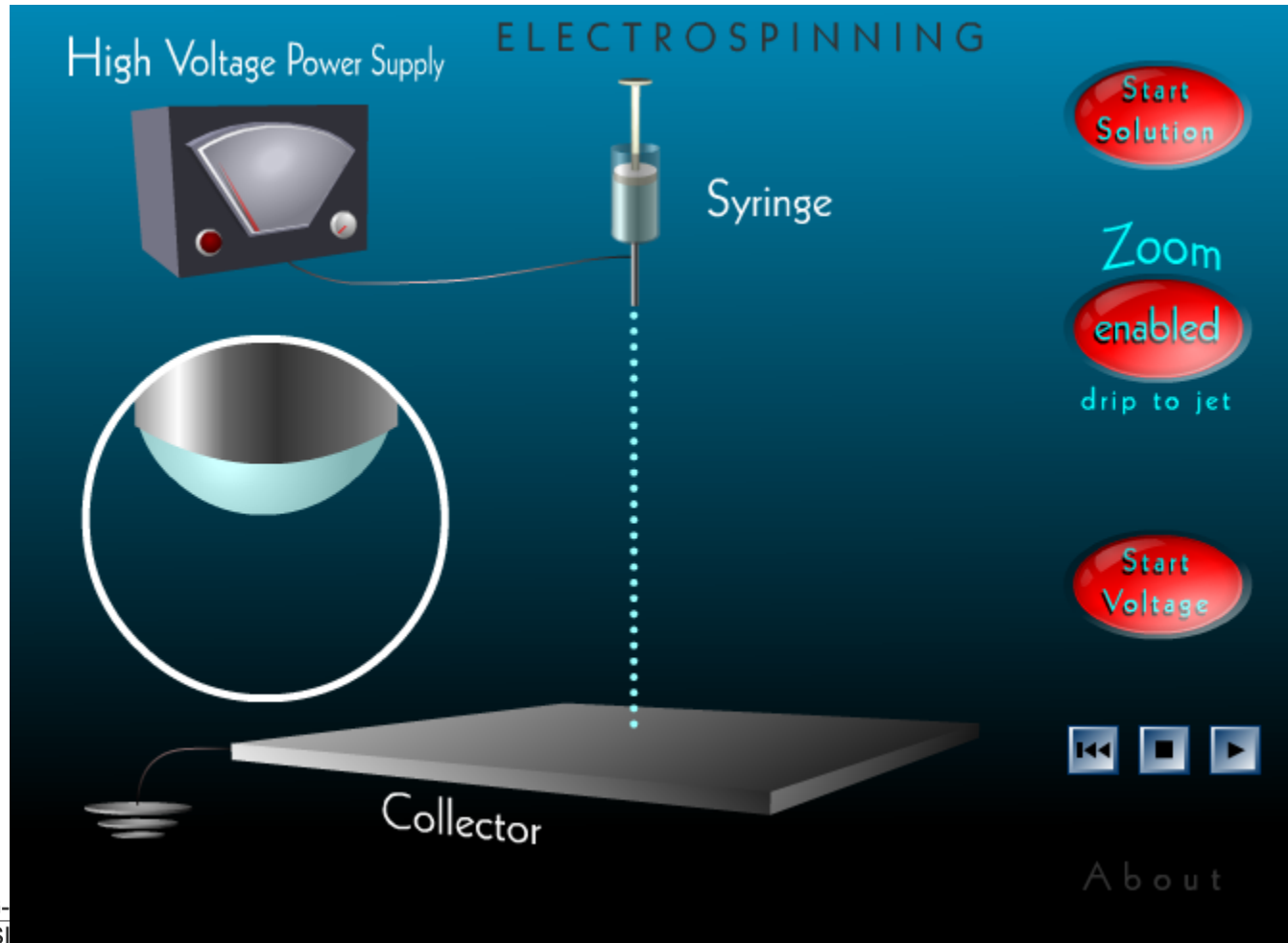
Electrospinning

Basics and Setup



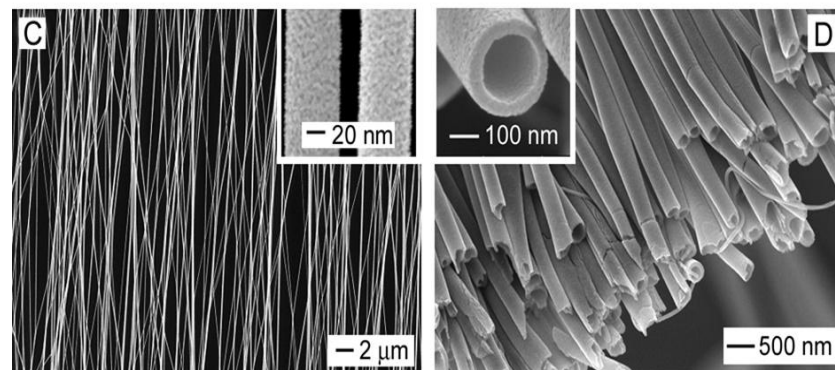
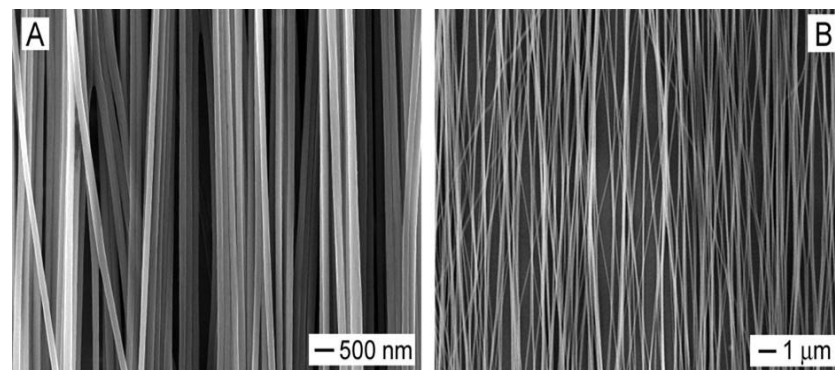
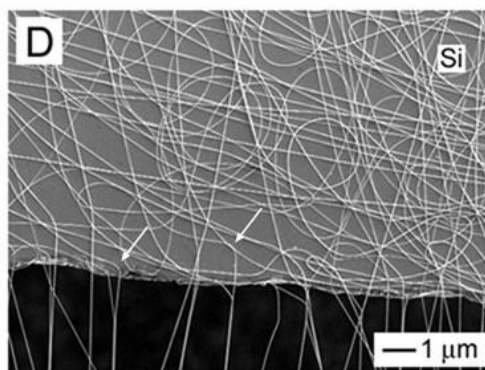
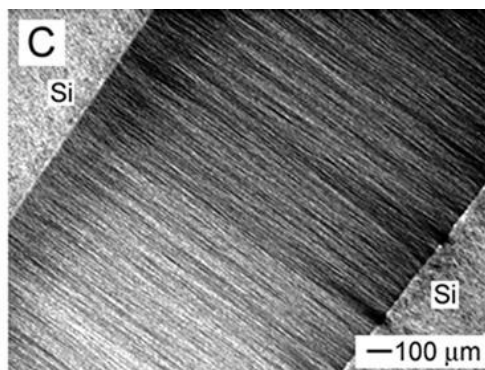
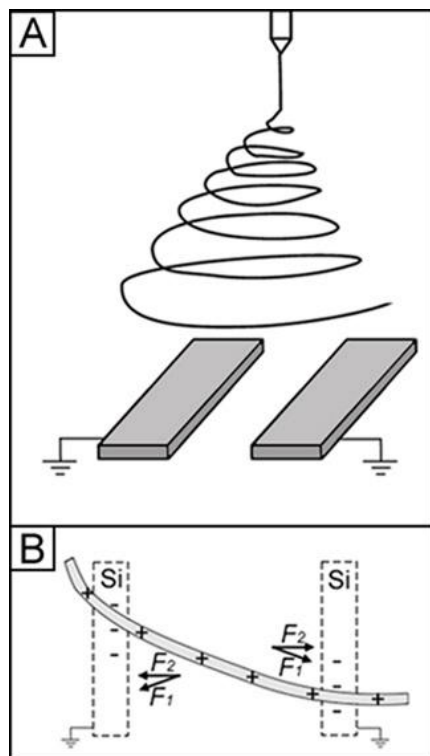
Electrospinning

How does it work?



Literature review

Alignment of Fibers



Li, Wang & Xia, *Nano Lett.* 2003, 3, 1167

Versatile materials by electrospinning

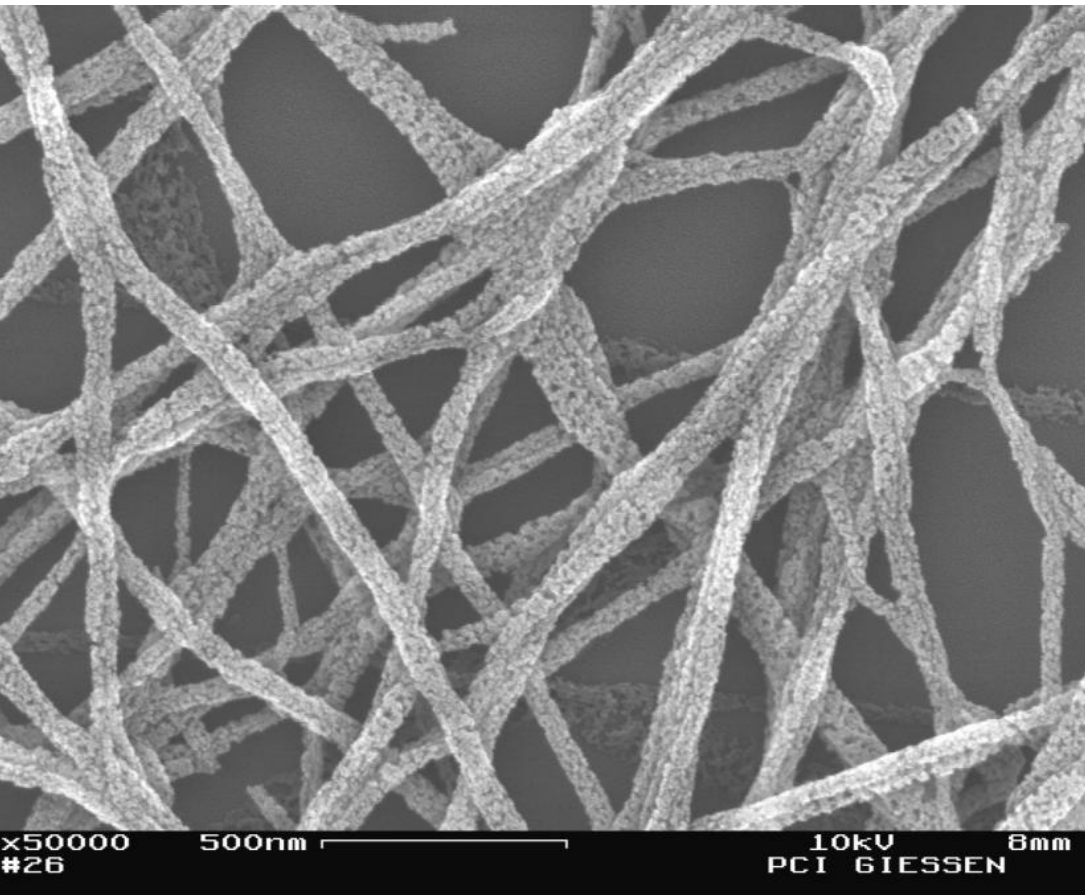
Thick mats



Thin coatings



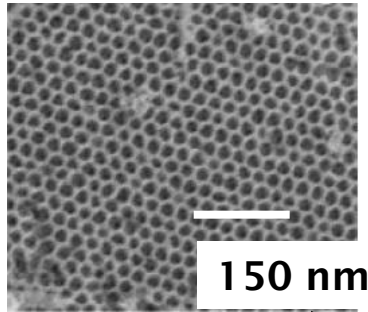
Possible benefits for medical applications



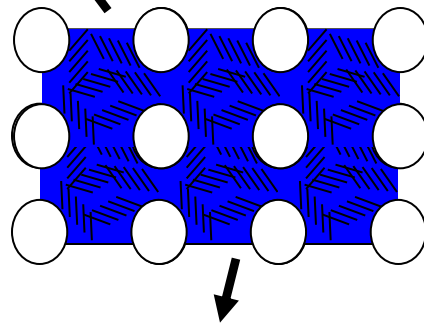
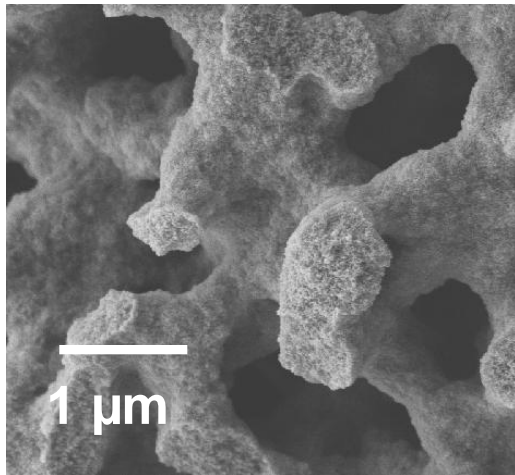
- **Electrospinning allows the generation of mats of reasonable mechanical stability**
- **Generation of internal porosity possible**

Generation of diverse pore structures

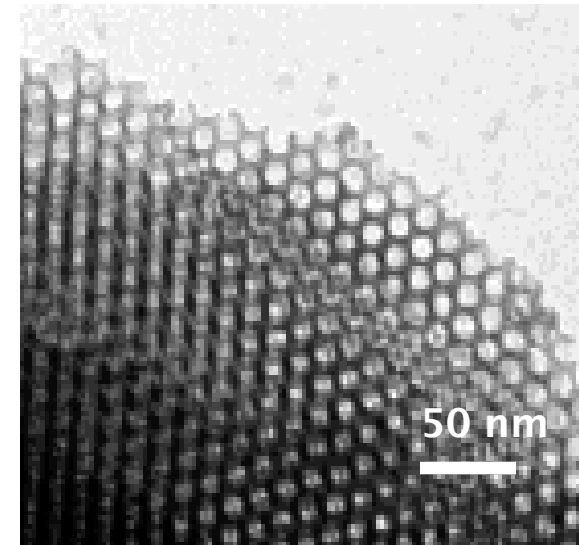
SMALL
polymer-colloids
(30 nm)



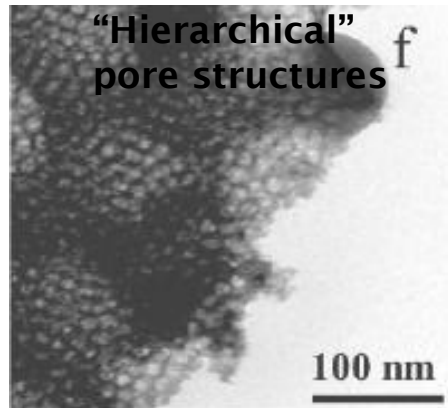
Polymer-
"sponge phases"



Lyotropic Blockcopolymer-
Mesophases

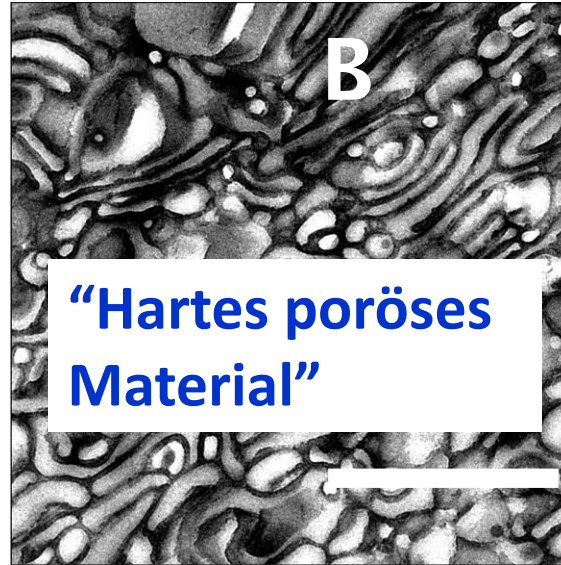
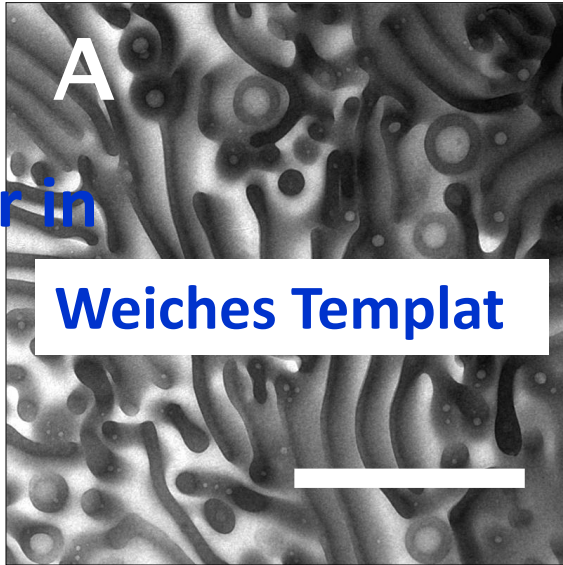


"Hierarchical"
pore structures



The principle of nanocasting

Elektronenmikroskopische Aufnahmen



**Nanoporöses
SiO₂**

**Skala:
1 Mikrometer**

**Polymer in
Wasser**